Intermediate valence in $Tm_xY_{1-x}Se$ using M_V x-ray absorption spectroscopy

W. D. Brewer, G. Kalkowski, and G. Kaindl
Fachbereich Physik, Freie Universität Berlin, Germany

F. Holtzberg
IBM Thomas J. Watson Research Center, Yorktown Heights, New York 10598

(Received 22 April 1985)

We have applied x-ray absorption spectroscopy (XAS) in the region of the Tm M_V edge to study the intermediate-valence behavior of the Tm ions in the series of mixed chalcogenides $Tm_xY_{1-x}Se$, with $0.004 \leq x \leq 1$. The clearly distinguishable spectral features resulting from divalent and trivalent Tm ionic states can be fitted with good accuracy to yield the mean Tm valence $\bar{v}$. We discuss the precision of the resulting values critically and consider the surface sensitivity of the technique. The results for concentrated Tm_xSe are in good agreement with lattice-constant systematics. In the dilute materials, we confirm the intermediate valence of Tm down to $x=0.4$ at. % and find $\bar{v}$ to be nearly constant below $x=20$ at. %, but to be lower than in TmSe.

I. INTRODUCTION

The thulium monochalcogenides TmX, with X=S, Se, or Te, exhibit an interesting variety of behavior with respect to the Tm ions and have been the subject of considerable study.[1,2] In TmS the bulk-Tm valence is 3+, while the surface atomic layer undergoes a valence transition to the divalent state.[3] In stoichiometric TmTe the bulk ions are divalent.[4] Tm_xSe exhibits mixed valence in the bulk[5] and shows a divalent surface.[3] The value of its bulk mean valence is sensitive to the exact stoichiometry x, and ranges from $\bar{v}=3$ for $x=0.85$ to about 2.75 for $x=1.05$.[6-8] Significant discrepancies between the bulk mean valence as derived from lattice-constant systematics and from magnetic and spectroscopic measurements have been reported,[6,8,9] with the latter for the most part showing valences 0.15—0.2 units lower. This compound is also unusual for an intermediate-valence material in that it orders antiferromagnetically below about 3.5 K;[10] both the integral-valence ions (Tm^{2+} and Tm^{3+}) have nonvanishing magnetic moments, in contrast to most candidates for mixed valence. Regarding the question of whether the mixed valence in this material is a collective phenomenon or a single-ion property, studies of an isomorphic series of compounds in which the Tm has been diluted by replacement with another ion, e.g., $Tm_xY_{1-x}Se$, are of special interest and several investigations of this system at dilutions of $x=0.05$ and below have been reported.[6,11-13] No strong systematic deviations in $\bar{v}$ as determined by different methods have been seen in the dilute system; however, precise valence determinations are generally difficult, especially at low Tm concentrations, and considerable scatter is seen. The general trend[6] is for $\bar{v}$ to decrease somewhat with decreasing x to about $x=0.20$, then to remain roughly constant.

We have previously pointed out the advantages of x-ray absorption spectroscopy (XAS) in the region of the M_{IV},M_V edges for the investigation of rare-earth mixed valence, particularly in the heavier rare earths with their well-localized $4f$ electrons.[14] Here, we give details of a study of the system $Tm_xY_{1-x}Se$ for $0.004 \leq x \leq 1$, employing M_V XAS detected by total electron yield from single-crystal samples in an ultrahigh vacuum (UHV), using synchrotron radiation as a source of x-ray photons in the required energy range near 1500 eV.[15]

In Sec. II we describe the experimental details. Section III treats the data analysis, in particular, the fitting of the experimental XAS spectra, which is important for the evaluation of the bulk mean valence of the samples. The results are presented in Sec. IV; they are discussed critically and in comparison to the results of other methods of valence determination in the Conclusion, Sec. V.

II. EXPERIMENTAL

Samples of Tm_xSe and Tm diluted in YSe were grown as single crystals by methods described previously.[6,16] The pieces used in these experiments had the form of rectangular prisms, typically 3—4 mm on a side. They were mounted by gluing the back face onto a Ta plate with conductive, UHV-compatible epoxy, then surrounding the sides of the crystal with a setting made of spot-welded Ta foils. The setting served to protect the sides of the crystal from the photon beam, so that only the cleaved surface was exposed and contributed to the signal. Several such samples were mounted on a manipulator in a UHV chamber equipped with a crystal cleaver. They could be moved into the cleaver, cleaved above the Ta setting, and returned to position in the photon beam within a short time. Cleaves were done at a typical chamber pressure of 1×10^{-10} Torr. Usually a trial cleave was performed a few millimeters above the setting, and after recording several spectra, a final cleave was made just at the height of the setting. The spectra of all but the most dilute samples were insensitive to exposure to the chamber pressure for several hours. Spectra were typically recorded for up to one hour after cleaving; a usual spectrum required 20 min measuring time.

Studies of the effects of oxygen exposure were performed to determine the surface sensitivity of the mea-

surements. For this purpose, the chamber was flooded with research-grade oxygen to 1×10^{-8} Torr for an appropriate time, after which the ion pump was restarted, giving a rapid pressure decrease to the 10^{-10}-Torr range.

Monochromatized x-ray photons were provided by the double-crystal monochromator JUMBO (Refs. 17 and 18) at Stanford Synchrotron Radiation Laboratory (SSRL), using beryl($10\bar{1}0$) crystals. The monochromator throughout was optimized at each energy setting using an analog-digital maximum search routine.[18] The input flux was determined by measuring the photocurrent I_t from a high-transmission Ni grid, and the output flux was measured as total electron yield from a gold grid, detected by a bare channeltron in current-sensitive mode (I_0). A similar channeltron was used to record the total electron yield (I_s) from the samples. Typical dark currents were 2 orders of magnitude smaller than the signals from these channeltrons, and were compensated using the zero offset of the current amplifiers at the beginning of each experiment. The noise in the spectra is thus due only to counting statistics and to fluctuations in the beam position and intensity, and to stray light passing through the monochromator; beam-intensity fluctuations are, to first order, cancelled by normalizing the measured sample photocurrent I_s to the corresponding beam intensity I_0. The variations in I_0 with photon energy were recorded and spectra with large variations were not used for data analysis. The photon beam could be made visible at the sample position using a fluorescent screen, and the size and shape of the beam were adjusted with collimators to optimize the signal for each sample.

The instrumental broadening of the absorption spectra due to the finite energy resolution of the monochromator could be determined by recording rocking curves using the I_0 detector as a monitor of the monochromator output. These curves must be recorded at several energies in the region of interest and repeated at frequent intervals, since the shape and width of the rocking curves from beryl crystals exposed to a relatively intense x-ray flux may change with time, and the width is in any case energy dependent. Fitting of the rocking curves allows the instrumental broadening to be taken precisely into account when analyzing the experimental spectra. Figure 1 shows a typical rocking curve in the energy range of the Tm M_V absorption threshold. These were best fit using a superposition of about 50% Gaussian and 50% Lorentzian line shapes with overall width (full width at half maximum) of 0.95 eV near a photon energy of 1450 eV. The rocking curves were asymmetric, being about 40% wider on the low-energy side.

After completion of a series of experiments, the cleaved crystal faces were analyzed by x-ray diffraction and by electron microprobe analysis to determine the lattice constants and the compositions. Quoted concentrations for Tm are accurate to $\pm5\%$ down to 0.5 at. % concentration, thereafter to $\pm10\%$ (95% confidence level). Some of the samples used in this work have also been studied by other techniques as will be mentioned below.

III. CURVE FITTING AND DATA ANALYSIS

An important aspect of this work lies in the relatively simple spectral signatures obtained from Tm^{2+} and

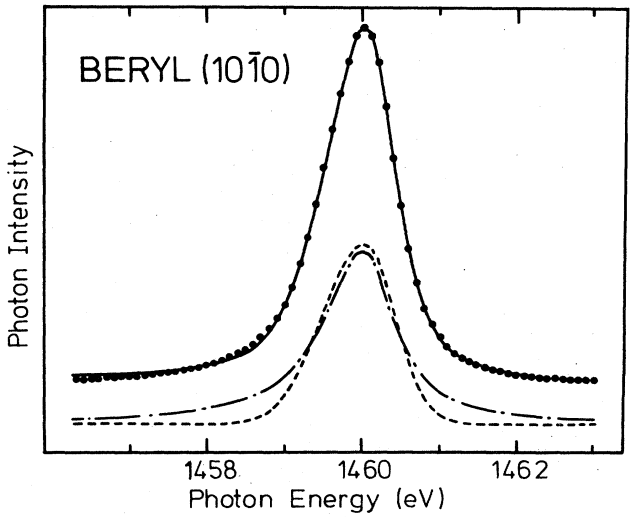

FIG. 1. Experimental rocking curve of the double-crystal monochromator at an energy near the Tm M_V edge. The solid line is a fit to the experimental points using a superposition of Gaussian and Lorentzian line shapes as indicated below (dashed and dashed-dotted curves).

Tm^{3+}, which allow precise curve fitting and determination of the ratio of the concentration of Tm^{2+} to Tm^{3+}. The Tm^{3+} XAS spectrum in the M_{IV},M_V region was studied by Belrhmi-Belhassan *et al.*[19] using x-ray transmission through 200—300-Å films of Tm and Tm_2O_3. They found good agreement with the calculated energy positions of the lines in the Tm^{3+} absorption multiplet, but were not able to make precise comparisons of the peak intensities due to saturation effects in the relatively thick samples. Therefore, they made no effort to fit the spectra obtained with calculated curves. In the present measurements, the sampling depth in the crystals is of order 50 Å or less, so that the observed relative line intensities should be reliable. Our values for the properties of the triplet of lines observed from trivalent Tm ($3d^{10}4f^{12}\rightarrow3d^{9}4f^{13}$) are summarized in Table I and compared there to those of Refs. 19 and 20.

The absolute energy calibration of the monochromator was determined by measuring the positions of the K edge from MgO and L edges from Ni and Cu samples and has an uncertainty of about ±2 eV. The energy scales of the Tm spectra were shifted linearly to give agreement of the most intense line from Tm^{3+} with that quoted in Ref. 19, 1462.2 eV. Within an energy range of 50 eV, the relative energies are accurate to better than ±0.1 eV and all fits give energy positions reproducible to this accuracy. Figure 2 shows M_{IV} and M_V spectra of TmF_3, Tm_2O_3, and $TmAl_2$, in which the Tm ions are trivalent. These spectra were fit with Lorentzian lines, which we broadened by convolution with experimental rocking curves to take account of the finite instrumental resolution.

The natural linewidth of the $3d\rightarrow4f$ resonance lines is determined by the $3d$ core-hole lifetime and is about 1.3 eV for the M_V lines;[20] the M_{IV} line is further broadened by Coster-Kronig transitions and autoionization processes.[21] This single line has an intensity less than 10% of

TABLE I. Observed energy shifts, linewidths, and relative intensities of the two weaker lines in the M_V triplet from Tm^{3+}. The most intense line, at 1462.2 eV, is taken to have relative intensity 1.0. The weak, broadened single M_{IV} line is also included.

Sample	E_2 (eV)	E_3 (eV)	FWHM (eV)	I_2	I_3	$I_{M_{IV}}$
Theory[a]	−2.1	+2.5	1.4	0.32	0.20	0.10
Tm, Tm_2O_3[a]	−2.0	+2.7	1.3[b]			
TmF_3[c]	−1.98	+2.75	1.29	0.44	0.165	0.066
Tm_2O_3[c]	−2.04	+2.72	1.55	0.44	0.16	0.077
$TmAl_2$[c]	−2.08	+2.67	1.45	0.45	0.18	
TmS[c]	−2.13	+2.76	1.41	0.445	0.15	
TmSe[c]	−2.20	+2.75	1.30	0.455	0.17	
TmTe[c]	−2.06	+2.70	1.33	0.46	0.15	

[a]From Ref. 19.
[b]From Ref. 20.
[c]This work.

that of the strongest line in the M_V triplet, as may be seen in Table I.

For the fits indicated in Fig. 2, an asymmetry of the Lorentzian lines was allowed. The Lorentzian linewidths, the instrumental broadening, and the asymmetries were held equal for all three lines in the Tm^{3+} M_V subspectrum. In addition, a constant background and a weak edge structure represented by an arctangent function were allowed for in the fits. The overlap between the $3d$ core levels and possible nf, mp continuum final states ($n \geq 5$, $m \geq 6$) is small, especially since the former lie outside the centrifugal barrier; the edge jump in the M_V region is thus hardly detectable in absorption measurements. The bare channeltrons used in this work, however, show enhanced sensitivity to threshold electrons,[22] which may explain the presence of a weak edge-like structure in the present electron-yield spectra. The edge is found to be relatively more intense in the spectra of dilute materials, as will be seen below. However, since the trivalent multiplet could be fit well in all cases while holding the relative intensities of the three lines constant, we believe the influence of the edge structure on the determination of the ratio of the intensity of the Tm^{2+} line to that of the Tm^{3+} triplet, $I(Tm^{2+})/I(Tm^{3+})$ to be minimal. This was verified by varying the parameters used for fitting the edge structure (width, amplitude), which showed the intensity ratios to be insensitive to the fit details. The spectra could also be fit satisfactorily using Fano-line profiles. The χ^2 values for the fits were comparable to those for the Lorentzian fits; typical values of the asymmetry parameter q were ≥ 30.

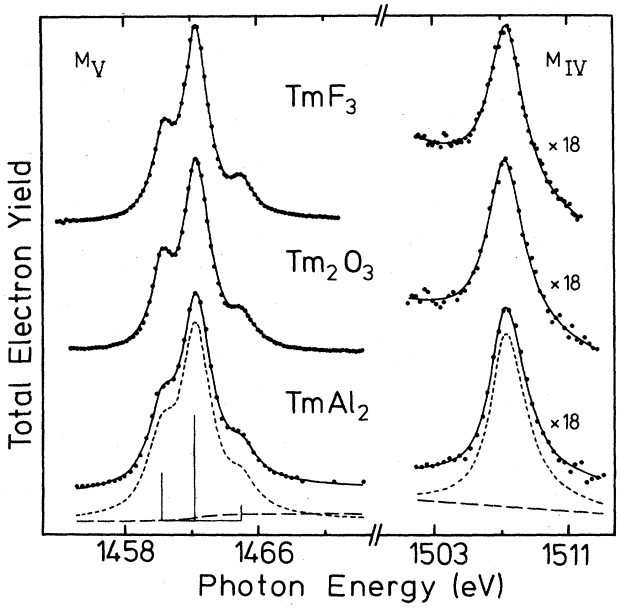

FIG. 2. Spectra of three trivalent thulium compounds (dots). The solid curves indicate fits obtained using a triplet of lines (bar diagram at bottom of figure). Each line is represented by a Lorentzian, broadened for instrumental resolution, and the lines are summed to give a synthetic spectrum (dashed curve). A typical background function is also shown (long-dashed curve). The spectra on the right show the single line from Tm^{3+} near the M_{IV} edge.

Samples containing divalent thulium show an additional single peak in the M_V region, about 3.3 eV below the center of gravity of the Tm^{3+} M_V triplet, and no additional absorption in the M_{IV} region (Fig. 3). This single line is expected due to the $3d^{10}4f^{13} \rightarrow 3d^9 4f^{14}$ transition originating from Tm^{2+}. Here, the final state has a filled $4f$ shell, which excludes exchange interactions with the $3d$ core holes and therefore leads to an unsplit line. A transition in the M_{IV} region ($3d_{3/2}$) is not allowed by the dipole-selection rule, considering the $^2F_{7/2}$ ground state. The shift of the Tm^{2+} M_V line to lower energies relative to the center of gravity of the transitions from Tm^{3+} results from the difference in the $4f$-$3d$ hole Coulomb interaction energies and the Coulomb correlation energy between the $4f^{13}$ and $4f^{14}$ states.[23] The former lowers the overall energy of the $4f^{14}$ final state resulting from divalent Tm ions, while the latter raises its energy relative to the $4f^{13}$ final state from trivalent Tm. Since the former energy is several eV larger in magnitude, the net effect is a lowering of the divalent transition energy by about 3 eV, as observed. The corresponding shift in the $4d \rightarrow 4f$ spectra is only 2 eV,[9] while it is about 8 eV in the $2p \rightarrow 5d, 6s$ excitation spectra observed in L_{III} XAS.[24]

In fitting the spectra, we held the width and asymmetry of the divalent line at the same values as those of the

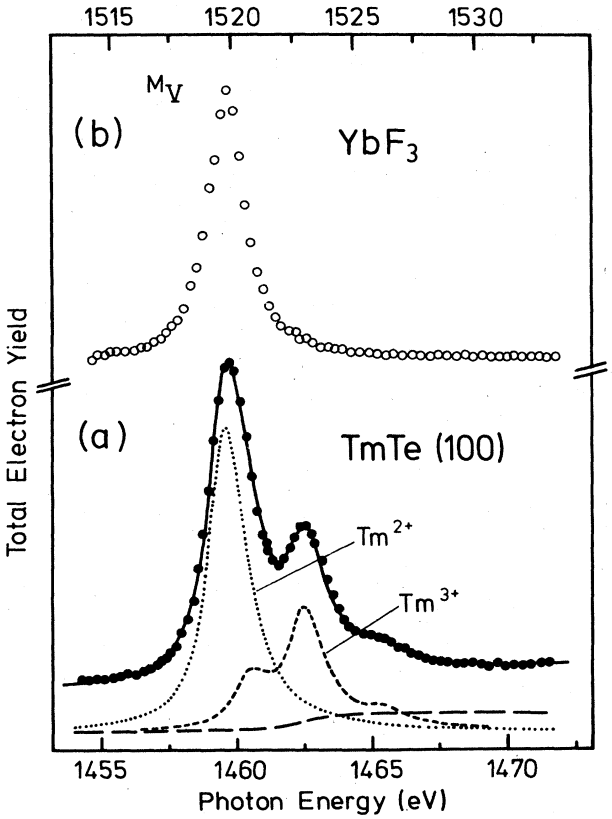

FIG. 3. (a) M_V spectrum obtained from a freshly cleaved TmTe crystal. It consists of a superposition of trivalent (dashed) and divalent (dotted) features. Again the solid line is a fit to the data points. (b) Comparison of the divalent M_V spectral feature from TmTe with the M_V spectrum of isoelectronic, trivalent Yb (upper energy scale).

trivalent triplet, allowing only the position and amplitude of the line to vary as free parameters. The energy position was quite reproducible over the range of Tm valences and concentrations studied. The significant quantity for valence determination is the ratio of the intensity of this single divalent feature to that of the trivalent triplet. The statistical errors in this quantity as obtained from the fit procedure were in general rather small, typically a few percent. In order to determine the range of systematic errors, we carried out several series of fits in which certain parameters were held constant and compared the results. For example, since the experimental rocking curves had considerable Lorentzian character, some of the spectra were also fitted using pure Lorentzian line shapes, broadened by both the $3d$ core-hole lifetime and by the instrumental resolution. These fits yielded about the same χ^2 values as the Gaussian-broadened ones, with typical overall linewidths being about 1.7 eV. Different assumptions about line asymmetry and background were also compared. The range of values resulting from these different fit procedures is included in the quoted errors for the Tm mean valences given below.

Figure 3(a) shows the fit to a spectrum obtained from the cleaved (100) surface of a TmTe single-crystal sample. This material is divalent in an ideal crystal, but shows an admixture of trivalent sites depending on the local Tm environment in actual samples.[4,25] Furthermore, the surface is known to be rather sensitive to oxidation.[26] A large fraction of divalent ions may be seen to be present in the spectrum shown in Fig. 3. Detailed analysis of the spectra (described below) shows a Tm^{3+} concentration of about 22.5 at.%, which is in agreement with the systematics of Ref. 4, taking the measured stoichiometry of the sample surface into account; a microprobe analysis gave the formula $Tm_{0.92}Te$, and x-ray diffraction indicated a lattice constant a_0 of about 6.33 Å.

The pure divalent Tm absorption spectrum is obtained by subtracting the trivalent multiplet from the experimental data in Fig. 3(a). The resulting single line (dotted curve) is compared with the M_V absorption spectrum of YbF_3 shown in Fig. 3(b). The trivalent Yb ions in this compound are isoelectronic with divalent Tm and give essentially the same resonance curve, apart from a shift in the energy position and a different intrinsic linewidth.

Since the absorption spectra originating from divalent and trivalent thulium ions are well known and relatively simple, spectra of materials containing an unknown proportion of the two valence states may be fitted to give an accurate determination of the mean Tm valence. The quantity immediately resulting from such fits is the ratio of the intensity of the single divalent line to the total intensity in the trivalent triplet, which we denote by α. In order to calculate the bulk mean Tm valence, two points must be taken into consideration.

(i) The *a priori* absorption probability from the divalent and the trivalent initial states is not equal. The probability ratio is given by the ratio of the number of holes in the $4f$ shells before absorption (following the Starace sum rule[27]), multiplied by the squares of the transition matrix elements. We denote the probability ratio by f; the observed intensity ratio α must be multiplied by f to give the true ratio of initial state divalent ($4f^{13}$) to trivalent ($4f^{12}$) populations.

(ii) Some portion of the observed spectrum originates in the sample surface, due to the surface sensitivity of the total-electron-yield method. It is known from photoemission work[3,13] that the surface layer of Tm chalcogenide crystals undergoes a surface valence transition to the divalent state; the latter is thus overrepresented in the experimental spectrum and a correction must be applied to account for this surface contribution in order to obtain the true bulk mean valence. We define a surface-sensitivity parameter s to be the fraction of the spectral intensity originating from that portion of the sample (defined as "surface") which becomes divalent.

The factor f is determined as follows: The divalent initial state has one hole in the $4f$ shell, the trivalent state has two, so the sum rule gives $f=2$. This must be corrected for the fact that we fit only the M_V part of the spectra to obtain the ratio α, thus neglecting the single weak M_{IV} line from trivalent Tm. Taking the experimental intensity found for this line in trivalent compounds (Table I) we find $f_5=1.912(5)$ [where f_5 applies only to the M_V spectrum (see Ref. 23)]. Finally, we multiply by the ratio of the squares of the dipole transition matrix elements from the divalent and trivalent states, calculated in

a relativistic atomic Hartree-Fock method by C. W. Clark.[28] Because of a slight contraction of the $4f$ orbitals in the trivalent ion, the overlap of the $3d$ and $4f$ shells is larger than in the divalent ion, resulting in a larger transition matrix element; the calculated ratio of the squares is 1.047, leading to a final value of 2.003(6) for f_5. (We note that this is slightly larger than the value used in a preliminary analysis of some of the present data,[14,29] due to neglect of the matrix-element correction in that work. The mean Tm valences quoted there are accordingly slightly higher than the present results.) It may be remarked that in most spectroscopic investigations of intermediate valence to date, matrix-element corrections have been entirely neglected.[3,8,9,24]

The surface sensitivity s must be determined experimentally. The simplest way to do this is to use a model compound with a well-established surface valence transition; such a case is offered by TmS. A single surface layer of atoms becomes divalent in this compound, so that the M_V spectrum of a freshly cleaved surface will show a divalent feature proportional to the fraction of the total signal originating in the surface layer. Fitting of such a spectrum allows the determination of the surface sensitivity. Alternatively, a second spectrum may be recorded from an oxygen-exposed surface, on which the divalent Tm ions have been oxidized to the trivalent state. Since the bulk is trivalent, the only effect of oxygen exposure is to eliminate the divalent signal from the surface layer and to restore a purely trivalent spectrum. Comparison of the spectra of freshly cleaved and oxidized surfaces will then allow the determination of s, even in intermediate-valence samples. An example is shown in Fig. 4, illustrating the analysis of the spectrum of a fresh cleave of the TmS(100) face. The relative intensity of the divalent peak, multiplied by f_5, leads to $s=0.06(2)$, i.e., 6% of the signal originates in the surface layer. Extrapolating linearly (which ignores scattering in subsurface layers and probably overestimates the sampling depth), we find that the total signal arises from about 16 atomic layers, corresponding to a sampling depth of roughly 50 Å (the average escape-depth to surface-thickness ratio, as used, e.g., in Ref. 9, is the reciprocal of our quantity s). Subtraction of the spectrum of an oxygen-exposed surface of the same sample yields consistent results for s.

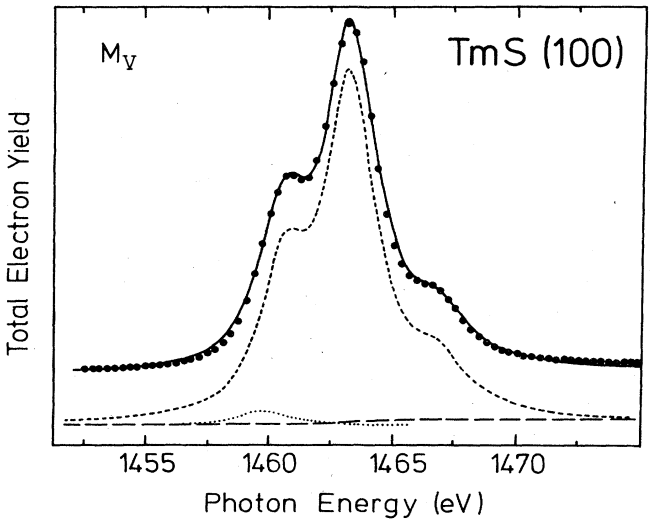

FIG. 4. Experimental M_V spectrum of a freshly cleaved (100) surface of TmS. The spectrum is dominated by a trivalent feature (dashed) from the bulk, but contains a weak divalent peak due to the surface valence transition (dotted curve). Superposition of the two curves plus background (long-dashed curve) gives the solid fit spectrum. The relative intensity of the divalent peak is a measure of the surface sensitivity of the method.

Having established the constants f_5 and s, we can proceed to a determination of the bulk mean valence $\bar{v}$ in intermediate-valence materials. The above value of s, obtained from bulk-trivalent TmS, represents a lower limit in this case, since in the intermediate-valence materials, more than one surface layer may undergo a valence transition, giving a greater "surface" signal as defined above. In addition, there is some indication[30] that the electron mean free path may be reduced in certain intermediate-valence materials, which would increase the surface sensitivity of the present technique. It is thus desirable to determine s separately for each sample. This can be done by oxygen-exposure experiments which, however, must be more selectively carried out than in the case of TmS, since one wishes to oxidize the divalent surface region only, but wants to avoid oxidation of the bulk. We have therefore studied the effect of varying oxygen exposures on cleaved $Tm_xY_{1-x}Se(100)$ surfaces. Figure 5 indicates the effect of an oxygen exposure of 2 L (1 L=one langmuir=10^{-6} Torr sec) on the M_V spectrum of nearly stoichiometric TmSe. In Fig. 5(a), a spectrum from a freshly cleaved crystal is shown, along with the decomposition into a triplet from trivalent Tm, a single divalent line, and a background curve. Figure 5(b) displays the spectrum of the same crystal surface after exposure to 2 L of oxygen, with an analogous spectral decomposition. The decrease in the relative intensity of the divalent feature on oxidation is apparent. Similar effects have been reported from valence-band x-ray photoemission spectroscopy (XPS) of TmSe in Refs. 3 and 9.

Figure 6 shows a series of oxygen exposures on a crystal of approximate composition $Tm_{0.05}Y_{0.95}Se$. The decrease in the intensity of the divalent feature can be seen qualitatively to saturate between 1.8-L and 4-L oxygen exposure. This is shown quantitatively in Fig. 7, where the change Δ^{3+} in the relative intensity of the *trivalent* signal compared to the freshly cleaved surface, which results from a particular oxygen exposure, is plotted against the exposure in langmuirs. At low exposures, the surface is only partially oxidized and the trivalent signal increases monotonically with increasing exposure. At some point a plateau is reached, corresponding to complete oxidation of the surface; the corresponding value of Δ^{3+} is simply equal to s as defined above. At very high exposures, we would expect Δ^{3+} to again increase as oxygen penetrates into the bulk and oxidizes the intermediate-valence Tm ions there; however, up to about 10 L we see no definite indication of this. As expected, the values of s for intermediate-valence materials are larger than for TmS (shown in Fig. 7 for

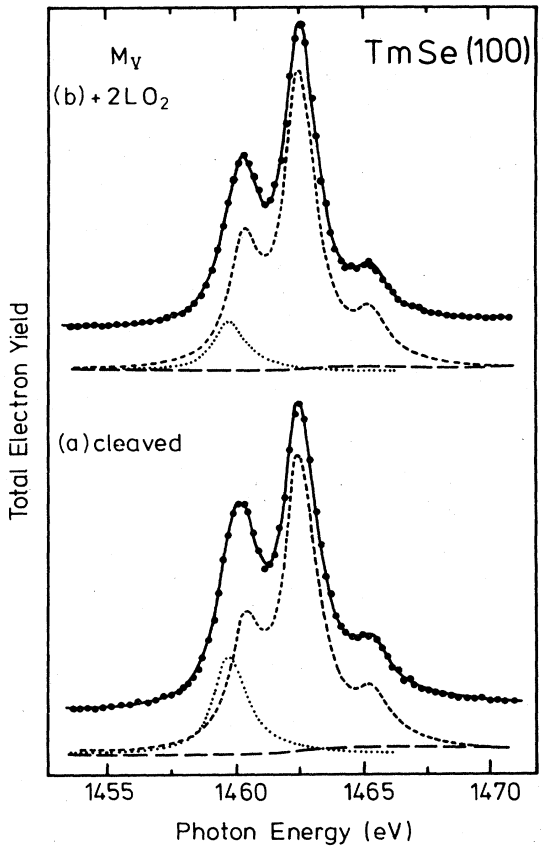

FIG. 5. Two M_V spectra of the same TmSe crystal, (a) from a fresh cleave and (b) after exposure of the same surface to 2 L of oxygen. The curves indicate the decomposition into trivalent and divalent subspectra. Note reduction of the latter on oxygen exposure.

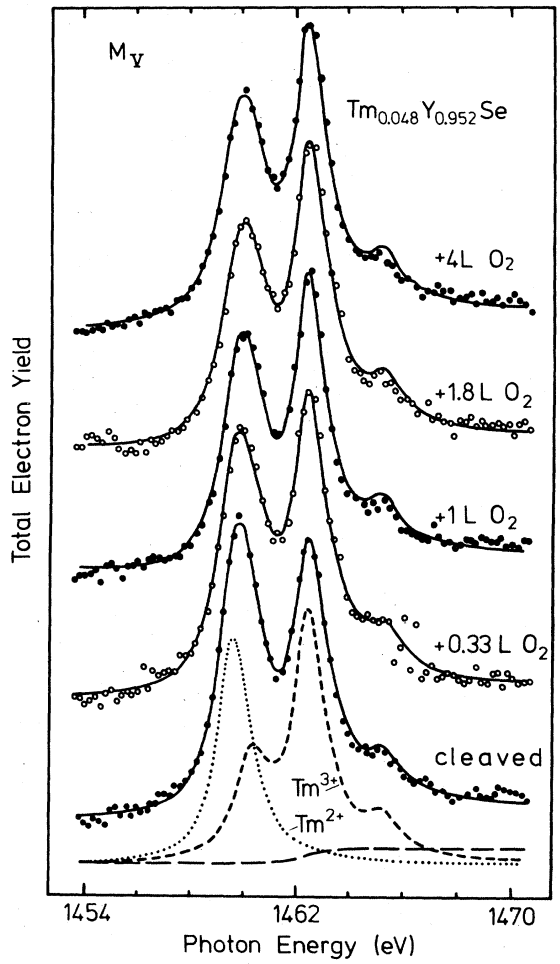

FIG. 6. Series of M_V spectra from the same (nominal 5 at. % Tm in Tm_xY_xSe) crystal, on the freshly cleaved surface (bottom) and after increasing O_2 exposures as indicated. Above about 2 L exposure, no further reduction in the divalent fraction is observed.

comparison). We take the value at the plateau determined from oxygen exposure of each sample to be equal to s, and use the maximum and minimum values of Δ^{3+} observed for small (≤ 0.5 L) and large (>4 L) oxygen exposures to give the range of probable values. This procedure is, in fact, rather conservative and probably overestimates the uncertainties in the surface correction. The quoted uncertainties in our derived mean valences include these extreme values for the surface correction.

With knowledge of f_5 and s, we can find $\bar{v}$ from the above definitions and the measured ratio α according to

$$\bar{v}=\frac{3+2\alpha f_5+s}{1+\alpha f_5} . \tag{1}$$

Alternatively, we can define β to be the measured intensity ratio of divalent to trivalent spectral features from an oxygen-exposed sample in the plateau region. This can then be combined with the ratio α from the clean surface to yield $\bar{v}$ directly:

$$\bar{v}=\frac{3+5\beta f_5+2(\alpha\beta f_5)^2}{1+2\beta f_5+(\alpha\beta f_5)^2} . \tag{2}$$

We have carried out such an analysis for several crystals

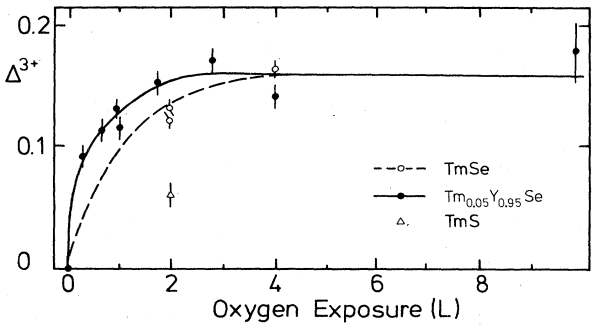

FIG. 7. Change Δ^{3+} in the relative intensity of the trivalent subspectrum compared to a freshly cleaved surface vs oxygen exposure in langmuirs, for two samples (TmSe, open circles; $Tm_{0.05}Y_{0.95}Se$, solid circles; TmS shown for comparison). Note saturation at higher exposures, indicating complete oxidation of the surface. The quantity Δ^{3+} is equal to the surface sensitivity s in the saturation region (see text).

of the series $Tm_xY_{1-x}Se$ with x varying from near 1 to less than 0.005. The properties of the samples studied are summarized in Table II. The results will be described in the next section.

IV. RESULTS FOR INTERMEDIATE-VALENCE COMPOUNDS $Tm_xY_{1-x}Se$

Spectra of clean and oxidized surfaces from a concentrated TmSe sample ($x \cong 1$) are shown in Fig. 5. As can be seen from the figure, the counting statistics are excellent and high-quality fits can be obtained as described in Sec. III. The principal source of uncertainty in the derived valences thus arises from the surface sensitivity s. Typical spectra and fits are shown over the whole concentration range of our studies in Fig. 8. It may be seen that the present technique is well suited for Tm concentrations below the 1% level. Here, uncertainties due to statistics are comparable to those introduced by the surface correction. The signal-to-noise ratios of the spectra, however, are still quite good, and measurements at even higher dilutions should be feasible with better photon-beam conditions (the present spectra were recorded using extremely low stored electron currents of only about 5 mA at 1.8 GeV).

In Table III the derived values of s from all the samples studied are set out, together with the resulting bulk mean valences. The quoted range of values takes into account statistical-fit errors, variations in fit parameters due to differing assumptions about line shapes and background, and the extreme assumptions regarding the uncertainty in the surface correction mentioned above. While it is difficult to assign a precise confidence level to these ranges, we believe they are very conservatively estimated and include all uncertainties resulting from analysis of the spectra, including surface corrections.

The reciprocals of the values for s in the table may be compared with the *average* of the escape-depth to surface-thickness ratio, $l/\delta s$, as determined in Ref. 9. In the present total-electron-yield method, the signal contains a weighted average over all electron energies shown in Fig. 6 of Ref. 9, as well as the low-energy inelastic electrons used in that work for partial-electron-yield photoabsorption measurements. The latter are more bulk sensitive and presumably have large values of $l/\delta s$. Our values from the table correspond to $l/\delta s$ of about 6—9, which is nearly twice the average value in the energy range 50—1200 eV reported in Ref. 9; this result is reasonable, given the contributions from inelastically scattered electrons in our method.

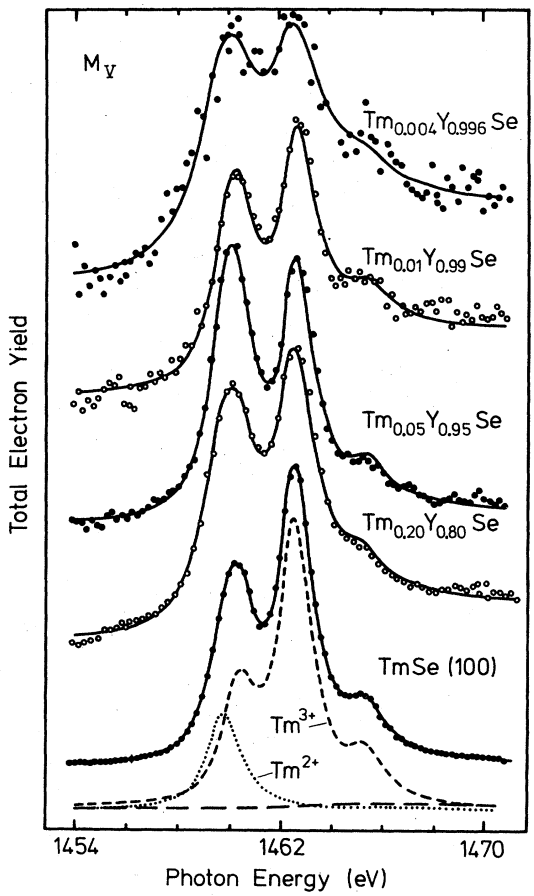

FIG. 8. Series of M_V spectra of freshly cleaved surfaces of TmSe and increasingly diluted Tm in YSe. A typical spectral decomposition is shown at bottom. The solid lines are the resulting fits.

We note that the value for $\bar{v}$ of the most dilute sample in Table III is to be regarded as an upper limit. This is not due primarily to difficulties associated with the low Tm concentration, but rather to the shape of this particular sample, which made it impossible to obtain a cleave with the photon beam not also striking parts of the uncleaved surface. For all the other samples, several spectra

TABLE II. Properties of samples studied in this work.

Sample designation	Nominal composition	Measured[a] composition	Measured[b] a_0 (Å)
1	TmSe	$Tm_{0.96}Se$	5.693(2)
2	TmSe	$Tm_{0.97}Se$	5.685(1)
3	TmSe	$Tm_{0.96}Se$	5.685(1)
4	$Tm_{0.2}Y_{0.8}Se$	$Tm_{0.207}Y_{0.753}Se$	5.724(1)
5	$Tm_{0.05}Y_{0.95}Se$	$Tm_{0.046}Y_{0.885}Se$	5.721(1)
6	$Tm_{0.01}Y_{0.99}Se$	$Tm_{0.009}Y_{0.887}Se$	5.720(2)
7	$Tm_{0.005}Y_{0.995}Se$	$Tm_{0.004}Y_{0.923}Se$	

[a]Using electron microprobe analysis on cleaved surfaces.
[b]By x-ray diffraction on cleaved surfaces after the XAS measurements.

TABLE III. Derived mean valences for TmSe and Tm diluted in YSe. The errors in the surface sensitivity s are obtained from plots like that of Fig. 7 and represent the extreme values observed for each sample.

Sample	Nominal composition	s	$\bar{v}$	$\bar{v}$ from[a] a_0
1	TmSe	$0.11^{+0.08}_{-0.04}$	$2.80^{+0.07}_{-0.03}$	2.825±0.005
2	TmSe	$0.13^{+0.08}_{-0.04}$	$2.81^{+0.07}_{-0.03}$	2.85 ±0.005
3	TmSe	$0.12^{+0.08}_{-0.05}$	$2.81^{+0.07}_{-0.04}$	2.85 ±0.005
4	$Tm_{0.2}Y_{0.8}Se$	$0.16^{+0.08}_{-0.04}$	$2.62^{+0.06}_{-0.02}$	2.70 ±0.03
5a[b]	$Tm_{0.05}Y_{0.95}Se$	$0.12^{+0.08}_{-0.04}$	$2.53^{+0.04}_{-0.02}$	2.80 ±0.12
5b[b]	$Tm_{0.05}Y_{0.95}Se$	$0.15^{+0.06}_{-0.04}$	$2.53^{+0.04}_{-0.02}$	
6	$Tm_{0.01}Y_{0.99}Se$	$0.11^{+0.06}_{-0.04}$	$2.63^{+0.05}_{-0.02}$	
7	$Tm_{0.005}Y_{0.005}Se$	$0.15^{+0.07}_{-0.04}$	$2.55^{+0.05}_{-0.02}$	

[a]Calculated using the correlation of Ref. 6.
[b]Samples 5a and 5b are different pieces of the same crystal.

were recorded on the cleaved surfaces, with adjustment of the sample and photon-beam position between measurements; in all cases, the resulting spectra were consistent within fit errors. The two values quoted for the $x=0.048$ sample were, in fact, obtained nearly a year apart in different experimental runs using different pieces of the same original crystal; their excellent agreement lends confidence in the experimental procedure and data analysis.

V. DISCUSSION AND CONCLUSIONS

A. Concentrated TmSe

It has been noted by various authors that systematic differences exist between determinations of the bulk mean valence of concentrated Tm_xSe samples based on lattice-constant systematics and on many other methods, including photoelectron spectroscopy, magnetic susceptibility, and L_{III}-edge XAS.[6,8,24] Some possible reasons for these discrepancies were suggested in Ref. 8.

The situation is summarized in Fig. 9, which is similar to a figure shown in Ref. 8, but contains newer data points, including those from the present work. The solid line in the upper part of the figure indicates the correlation between valence and lattice constant inferred from Ref. 6; the shading indicates the range covered by the somewhat different correlations quoted in Refs. 7 and 8. Our data points for three samples are shown as solid squares and may be seen to agree with the lattice-constant data. Valences determined by other methods fall into several groups: photoemission (XPS) (Refs. 3 and 8) and early susceptibility measurements[2] are well described by the dashed line, with which earlier L_{III} XAS (Ref. 24), recent $4d$ ($N_{IV}N_V$) XAS (Ref. 9) and bremstrahlung isochromat spectroscopy (BIS) (Ref. 31) results also agree reasonably well, although they give systematically higher valences. A somewhat steeper dependence (dashed-dotted line) is found from the correlation given in Ref. 33, which is based on all available magnetic data. Finally, recent L_{III} XAS results[33,34] fall between the areas bracketed above by the lattice constant and below by the XPS and susceptibility lines. Thus, agreement among the spectroscopic methods no longer seems to be as perfect as had earlier been supposed.[35]

The lattice-constant—valence correlations are based on the assumption of a linear variation of lattice constant with concentration between the divalent and trivalent extremes (Vegard's law). This linear variation has been called into question[36] and a model using the different compressibilities of divalent and trivalent materials has been proposed,[35] which leads to a curvature in the lattice-constant—valence correlation; this model predicts a valence for stoichiometric TmSe of about 2.63, well below

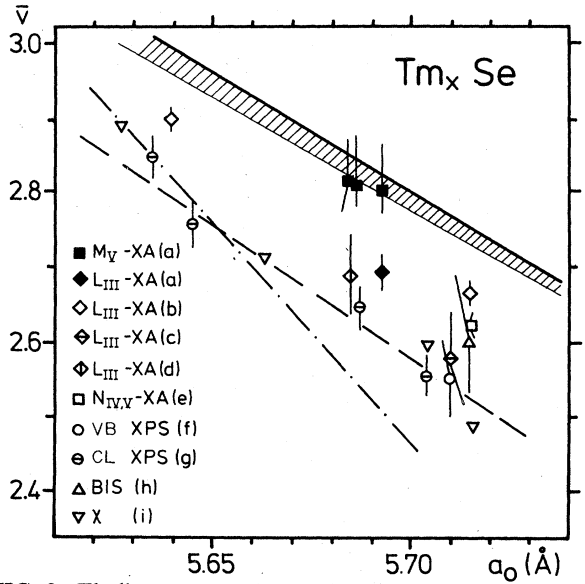

FIG. 9. Thulium mean valence $\bar{v}$ in Tm_xSe, as determined by various methods, vs lattice constant a_0. The upper solid line indicates the $\bar{v}$-a_0 correlation given in Ref. 6; the shaded region includes those of Refs. 7 and 8. The inverted open triangles (i) show the susceptibility data of Ref. 2. The remaining points represent spectroscopic data: (a), present work and Ref. 33; (b), Ref. 34; (c), Ref. 24; (d), Ref. 33; (e), Ref. 9; (f), Ref. 3; (g), Ref. 8; and (h), Ref. 31. The dashed line is a fit to the core-level (CL) XPS data points (g), which agree with susceptibility, valence-band (VB) XPS, BIS, and some L_{III} XAS data. The correlation found using all available magnetic data by Boppart (Ref. 32) is shown by the dotted-dashed line. The most recent L_{III} XAS [(a) and (b)] and $N_{IV,V}$ XAS (e) data fall in an intermediate region.

that expected from the present M_V XAS work and also lower than the most recent L_{III} XAS results. Although the model of Ref. 35 is a first step, it is not clear whether a calculation based on macroscopic lattice properties is applicable to microscopic intermediate-valence phenomena. We also note that a clearly linear behavior of lattice constant *versus* stoichiometry in TmSe over most of the range covered in Fig. 9 has been observed.[6,7,37]

In Ref. 32 extremely large discrepancies between valence (as indicated by the lattice constant) and by magnetic susceptibility in $TmSe_{1-y}Te_y$ in a certain range of y and pressure, which correlate well with the observed discrepancies in Tm_xSe for lower values of y, have been reported. In this case the variations are much too large to be explained by deviations from Vegard's law; while some part of the lattice-constant variation may be due to lattice effects (changing defect concentration), it seems likely that the electronic structure of the Tm ions must also play a role. Recently reported calculations by Jansen, Freeman, and Monnier,[38] using the full-potential linearized-augmented-plane-wave method in the local-density approximation, give convincing theoretical evidence that, while the major portion of the $4f$ electron density is atomiclike and localized on the Tm ions, a certain fraction (about 3%) is to be found in the interatomic regions, and that furthermore, both f-d and f-p (ligand) hybridization play an important role in determining the electronic structure of TmSe. Since the Se $4p$ electrons are primarily responsible for bonding, a change in their hybridization with the Tm $4f$ electrons will affect the bond lengths and thus the lattice constant. Such changes occur continuously with pressure or alloying as the f-d gap is closed, however, leaving the magnetic properties of the $4f$ shell largely unchanged until the gap closes completely. A discrete change in f-d hybridization then occurs, giving rise to a corresponding change in the Tm magnetic moment, as observed. This mechanism clearly has consequences for spectroscopic measurements as well. In particular, L_{III} XAS, with final states in the $5d$ shell, is likely to be more sensitive to hybridization effects than the present M_V method, where the excited electron is in a well-localized $4f$ final state.

In fact, we see no direct evidence of hybridization effects in our spectra: the Tm^{3+} triplet has the same peak intensities and positions from samples in which the Tm has a variety of different chemical environments. By contrast, the effects of $4f$-valence[39,40] or $4f$-ligand[41–43] hybridization *are* seen in the form of a collapse of the multiplet structure and changes of the multiplet envelope shape in the M_{IV},M_V spectra of Ce compounds.[23] The lack of such effects in the Tm spectra indicates that hybridization of the Tm $4f$ shell is too subtle to be observed directly by this method; this is, of course, an advantage for valence determination. We note that the results reported in Ref. 38 imply a certain amount of covalency in the Tm-Se bonding, which is in turn dependent on the effective Tm valence, so that the definition of the latter becomes imprecise and one should preferably speak of the ionicity of the Tm bonding.

Even if we do not admit such an explanation of the discrepancies observed between various methods of valence determination in TmSe, they must still be understood in terms of systematic errors or errors of interpretation. We note in this connection that the surface correction applied to the present results could not be responsible for the disagreement with XPS values: even if we make the hardly reasonable assumption of *no* surface sensitivity in our spectra, our observed values of the intensity ratio α would still have to be about 50% larger to obtain agreement. A measurement or fit error of this magnitude is most unlikely.

In summary, we find it improbable that the discrepancies between the present results and other spectroscopies used in studying TmSe are due to experimental or data analysis problems. The different spectroscopies (XPS, BIS, L_{III} XAS, and M_{IV},M_V XAS) may well be sensitive to different aspects of the $4f$ electronic structure. We find here among "high-energy" spectroscopies an interesting parallel to the different valence sampling observed in "low-energy" methods by Boppart and Wachter.[32]

B. Dilute Tm in YSe

An advantage of the present method is its combination of sensitivity and atomic specificity, allowing it to be applied to highly-diluted compounds or alloys. It has recently been demonstrated[34] that the standard L_{III} XAS technique is also applicable to Tm dilutions of order 0.2—0.3 at. % in the $Tm_xY_{1-x}Se$ system. The latter technique has the disadvantage of having a considerably more complex background which must be subtracted in fitting the experimental divalent-to-trivalent intensity ratio, and

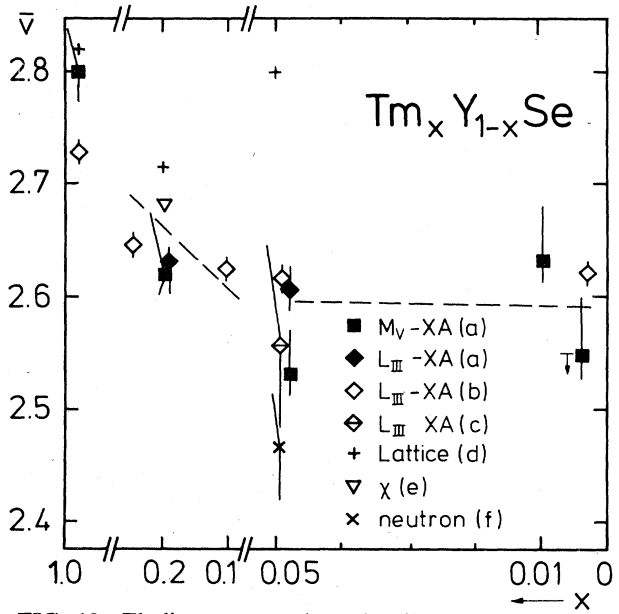

FIG. 10. Thulium mean valence in diluted Tm in YSe as a function of Tm concentration x. The lattice-constant correlation values (d) are from Refs. 6 and 34 and the solid squares (a) are from the present work. Note breaks in x scale. Recent L_{III} XAS data [(a), present work and Ref. 33; (b), Ref. 34], an earlier L_{III} XAS result [(c), Ref. 36], a susceptibility measurement [(e), Ref. 6]; and a neutron diffraction result [(f), Ref. 12] are also shown.

of utilizing powdered samples, which are more difficult to characterize than the clean surfaces used in the present work. Its sensitivity at high dilutions can, however, be increased by simply increasing the effective absorber thickness (until this is limited by parasitic absorption due to the other elements present in the sample). The two methods are complementary in providing spectroscopic information on the valence of lanthanide ions even at high dilutions, while being sensitive to somewhat different details of the electronic structure, since different angular-momentum components are involved. In addition, different sources of systematic errors are to be expected, so that results from the two methods should be compared whenever possible. This has now been done for the dilute Tm in YSe series. Figure 10 summarizes the data over the concentration range studied and compares the present results with those of Ref. 34 as well as other works. The results from the two spectroscopies are in reasonably good agreement and both methods show a moderate decrease of $\bar{v}$ in going from the concentrated compound to about 20 at. % Tm content, followed by a smaller gradual decrease as the Tm dilution increases. The intermediate valence of Tm ions down to very low concentrations is confirmed, implying that it is a single-ion effect.

As may be seen in Fig. 10, various methods of valence determination are in better agreement for the dilute samples than for concentrated TmSe. There is still a tendency for lattice-constant values to be systematically higher, but the differences are no longer significant. The uncertainties quoted for the XAS data of Ref. 34 seem extremely small and probably only reflect statistical-fit errors. If we take this into account, essentially all the data are in agreement, indicating a valence near 2.6, remaining roughly constant, over the concentration range $0.003 \leq x \leq 0.1$. Our data show a distinct rise in $\bar{v}$ near 1 at. % Tm concentration, which seems to be significant even outside the generous quoted errors. Whether this is physically meaningful or not must be decided by more detailed work at these low concentrations; we mention only that a similar anomaly in the lattice constant of dilute $Tm_xY_{1-x}S$ has been seen in preliminary work.[44]

In conclusion, we have applied M_V x-ray absorption spectroscopy using total-electron-yield detection and synchrotron-radiation excitation to the study of intermediate valence in a series of $Tm_xY_{1-x}Se$ compounds. The samples were single crystals, freshly cleaved in UHV and later characterized on the cleaved surfaces. The valences derived have uncertainties comparable to or smaller than those resulting from most other methods, even after allowing for surface effects. For concentrated samples, they are in good agreement with lattice-constant systematics and in reasonably good agreement with L_{III}-edge XAS data. Using dilute samples, we have demonstrated the applicability of the technique at high dilutions and confirm the intermediate valence of the dilute Tm ions. The simplicity of the data analysis and the success of the method are in part due to the nearly atomic character of the $4f$ electrons in these Tm compounds.

ACKNOWLEDGMENTS

We are grateful for the hospitality and support of the Lawrence Berkeley Laboratory, particularly to Professor D. A. Shirley, J. Barton, and W. Heppler. Assistance with the measurements was given by Dr. E. Paparazzo and by A. Schach v. Wittenau. We thank the SSRL staff for their support, especially M. Rowan and A. Waldhauer. Aid in preparing and characterizing our single crystals was provided by S. Kramer and F. Cardone of IBM, Yorktown Heights. This work was supported in part by the Bundesminister für Forschung u. Technologie, Project No. 05-256KA, and by the U.S. Department of Energy (Lawrence Berkeley Laboratory and SSRL).

[1]P. Haën, F. Lapierre, J. M. Mignot, R. Tournier, and F. Holtzberg, Phys. Rev. Lett. **43**, 304 (1979).

[2]B. Batlogg, H. R. Ott, E. Kaldis, W. Thöni, and P. Wachter, Phys. Rev. B **19**, 247 (1979).

[3]G. Kaindl, C. Laubschat, B. Reihl, R. A. Pollak, N. Mårtensson, F. Holtzberg, and D. E. Eastman, Phys. Rev. B **26**, 1713 (1982).

[4]H. R. Ott and F. Hulliger, Z. Phys. B **49**, 323 (1983).

[5]M. Campagna, E. Bucher, G. K. Wertheim, D. N. E. Buchanan, and L. D. Longinotti, Phys. Rev. Lett. **32**, 885 (1974).

[6]F. Holtzberg, T. Penney, and R. Tournier, J. Phys. (Paris) Colloq. **40**, C5-314 (1979).

[7]E. Kaldis and B. Fritzler, Solid State Chem. **14**, 95 (1982).

[8]G. K. Wertheim, W. Eib, E. Kaldis, and M. Campagna, Phys. Rev. B **22**, 6240 (1980).

[9]S.-J. Oh, J. W. Allen, and I. Lindau, Phys. Rev. B **30**, 1937 (1984).

[10]S. M. Shapiro, H. B. Møller, J. D. Axe, R. J. Birgenau, and E. Bucher, J. Appl. Phys. **49**, 201 (1978).

[11]A. Berger, P. Haën, F. Holtzberg, F. Lapierre, J. M. Mignot, T. Penney, O. Peña, and R. Tournier, J. Phys. (Paris) Colloq. **40**, C5-364 (1979).

[12]E. Holland-Moritz, J. Magn. Magn. Mater. **38**, 253 (1983).

[13]N. Mårtensson, B. Reihl, R. A. Pollak, F. Holtzberg, G. Kaindl, and D. E. Eastman, Phys. Rev. B **26**, 648 (1982).

[14]G. Kaindl, W. D. Brewer, G. Kalkowski, and F. Holtzberg, Phys. Rev. Lett. **51**, 2056 (1983).

[15]A preliminary report was given by G. Kalkowski, W. D. Brewer, G. Kaindl, and F. Holtzberg, in *Proceedings of the IVth International Conference on Valence Fluctuations Cologne, 1984* [J. Magn. Magn. Mater. **47-48**, 215 (1985)].

[16]F. Holtzberg, D. C. Cronemeyer, T. R. McGuire, and S. von Molnar, in Proceedings of the Fifth Materials Research Symposium NBS Special Publication No. 364, 1972, p. 637 (unpublished).

[17]J. Cerino, J. Stöhr, N. Hower, and R. Z. Bachrach, Nucl. Instrum. Methods **172**, 227 (1980).

[18]Z. Hussain, R. Umbach, D. A. Shirley, J. Stöhr, and J. Feldhaus, Nucl. Instrum. Methods **195**, 115 (1982).

[19]A. Belrhmi-Belhassan, R. C. Karnatak, N. Spector, and C. Bonnelle, Phys. Lett. **82A**, 174 (1981).

[20]R. C. Karnatak, J.-M. Esteva, and J. P. Connerade, J. Phys. B **14**, 4747 (1981).

[21]J. P. Connerade and R. C. Karnatak, J. Phys. F **11**, 1539 (1981).

[22]W. Eberhardt, J. Stöhr, J. Feldhaus, E. W. Plummer, and F. Sette, Phys. Rev. Lett. **51**, 2370 (1983).
[23]G. Kaindl, G. Kalkowski, W. D. Brewer, E. V. Sampathkumaran, F. Holtzberg, and A. Schach v. Wittenau, J. Magn. Magn. Mater. **47-48 48**, 181 (1985).
[24]H. Launois, M. Raviso, E. Holland-Moritz, R. Pott, and D. K. Wohlleben, Phys. Rev. Lett. **44**, 1271 (1980).
[25]E. Kaldis, E. Jilek, and H. Spychiger, J. Less-Common Met. **93**, 399 (1983).
[26]R. Suryanarayanan, G. Güntherodt, J. L. Freeouf, and F. Holtzberg, Phys. Rev. B **12**, 4215 (1975).
[27]A. F. Starace, Phys. Rev. B **5**, 1773 (1972).
[28]C. W. Clark (private communication); see also Ref. 23.
[29]G. Kaindl, G. Kalkowski, W. D. Brewer, B. Perscheid, and F. Holtzberg, J. Appl. Phys. **55**, 1910 (1984).
[30]C. Laubschat, G. Kaindl, W.-D. Schneider, B. Reihl, and N. Mårtensson (unpublished); see also Refs. 3 and 9.
[31]S.-J. Oh and J. W. Allen, Phys. Rev. B **29**, 589 (1984).
[32]H. Boppart and P. Wachter, in Proceedings of ASI on Moment Formation in Metals, Pearson College, Vancouver Island, 1983 (unpublished); also H. Boppart, J. Magn. Magn. Mater. **47-48**, 436 (1985); Phys. Rev. Lett. **53**, 1759 (1984).
[33]G. Schmiesster, W. Krone, G. Wortmann, and G. Kaindl (unpublished). These L_{III} XAS experiments were performed on the same samples used in this work employing both transmission through powders and fluorescence yield detection.
[34]P. Haën, F. Lapierre, J. M. Mignot, J. P. Kappler, G. Krill, and M. F. Ravet, in *Proceedings of the IVth International Conference on Valence Fluctuations, Cologne, 1984,* Ref. 15, p. 490.
[35]G. Neumann, R. Pott, J. Roehler, W. Schablitz, D. Wohlleben, and H. Zahel, in *Valence Instabilities,* edited by P. Wachter and H. Boppart (North-Holland, Amsterdam 1982), p. 87; D. Wohlleben, in Proceedings of ASI on Moment Formation in Metals, Pearson College, Vancouver Island, 1983 (unpublished).
[36]D. K. Wohlleben, in *Valence Fluctuations in Solids,* edited by L. M. Falicov, W. Hanke, and M. B. Maple (North-Holland, Amsterdam, 1981), p. 1.
[37]E. Kaldis, H. Spychiger, and E. Jilek, in *Proceedings of the IV International Conference on Valence Fluctuations, Cologne, 1984,* Ref. 15, p. 478.
[38]H. J. F. Jansen, A. J. Freeman, and R. Monnier, Phys. Rev. B **31**, 4092 (1985).
[39]O. Gunnarsson and K. Schönhammer, Phys. Rev. B **28**, 4315 (1983).
[40]J. C. Fuggle, F. U. Hillebrecht, J.-M. Esteva, R. C. Karnatak, O. Gunnarsson, and K. Schönhammer, Phys. Rev. B **27**, 4637 (1983).
[41]A. Fujimori, Phys. Rev. B **28**, 2281 (1983).
[42]S.-J. Oh, J. W. Allen, and B. Johansson, Bull. Am. Phys. Soc. **28**, 269 (1983).
[43]E. V. Sampathkumaran, G. Kalkowski, C. Laubschat, G. Kaindl, M. Domke, G. Schmiesster, and G. Wortmann, J. Magn. Magn. Mater. **47-48**, 212 (1985).
[44]F. Holtzberg (unpublished).